UWL REPOSITORY

repository.uwl.ac.uk

Comprehensive analysis of transcriptomics and metabolomics to understand the flesh quality regulation of crucian carp (Carassius auratus) treated with short term micro-flowing water system

This is the Accepted Version of the final output.

1 **Comprehensive analysis of transcriptomics and metabolomics to understand the flesh**

2 **quality regulation of crucian carp (*Carassius auratus*) treated with short term micro-flowing**

3 **water system**

4 Hongying Du[a, b]; Shanbai Xiong[a, b, *]; Hao Lv[a]; Siming Zhao[a, b]; Anne Manyande[c]

5

6 [a] Key Laboratory of Environment Correlative Dietology, Ministry of Education, College of Food

7 Science and Technology, Huazhong Agricultural University, Wuhan, Hubei, P.R. China

8 [b] National R & D Branch Center for Conventional Freshwater Fish Processing, Wuhan, Hubei

9 430070, P.R. China

10 [c] School of Human and Social Sciences, University of West London, Middlesex TW8 9GA, UK

11

12

13 ***** Corresponding author

14 **Shanbai Xiong**: Email: xiongsb@mail.hzau.edu.cn; Phone: 86-27-87288375;

15 **Abstract**

16 The short term micro-flowing purification system (STMFPS) has been shown to improve the flesh

17 quality of freshwater fish. However, few studies have focused on the involved underlying

18 mechanisms. This study explored the effect of STMFPS on the flesh quality of market-size

19 freshwater fish based on the combination of metabolomics and transcriptomics methods. The

20 UPLC-QTOF/MS based metabolomics method was utilized to screen metabolites and predict the

21 possible major metabolic pathways during different STMFPS treatment periods (0 d, 1 d, 5 d and 9

22 d). Furthermore, the transcriptomic data demonstrated that the differentially expressed genes

23 detected in crucian carp muscle were 2915,7852 and 7183 after 1 d, 5 d and 9 d STMFPS treatment.

24 Results showed that the TCA cycle, ornithine cycle, purine metabolism and amino acid catabolism

25 play important roles in improving the flesh quality of crucian carp. This study may help to

26 understand the mechanism of improving the flesh quality of aquatic products using STMFPS.

27

28 ***Keywords***: Freshwater fish, Mass spectrometry (MS); Genes; Metabolites; Principal component

29 analysis (PCA); Orthogonal partial least squares discriminant analysis (OPLS-DA)

30

1. Introduction

Crucian carp (*Carassius auratus*) is an omnivorous and important economic freshwater fish which is widely farmed in China (Ling et al., 2019), due to its palatability, fast growth rate, and high nutritional quality (Cui et al., 2020; Wu, 2020). The aquaculture of crucian carp has rapidly grown over the last two decades, and it has become one of the most important economic sources in China. Currently, high-density cultivation is the most popular method used for crucian carp production (Su, Luo, Jiao, & Wu, 2017). However, the rearing conditions or cultivation of microorganisms in aquatic environments could easily result in the accumulation of undesirable flavors in the fish, which in turn would affect to some extent the degree of acceptance by consumers of the crucian carp (Fuentes, Fernández-Segovia, Serra, & Barat, 2010; Rincón et al., 2016). In other words, the quality of crucian carp could have obvious disadvantages, such as loose muscle tissue, poorer taste *etc*. (Grigorakis, Taylor, & Alexis, 2003). In order to solve the poor quality of farmed freshwater fish under high-density cultivation, a variety of depuration treatments are used to improve the quality and acceptability of market-size fish before sales. The quality of numerous kinds of fish was significantly improved by depuration or purging and recirculating aquaculture systems, including halibut (Drake, DRAKE, Sanderson, Daniels, & Yates, 2010), atlantic salmon (Burr, Wolters, Schrader, & Summerfelt, 2012), rainbow trout (Schrader, Davidson, & Summerfelt, 2013), common carp (Zajic, Mraz, Sampels, & Pickova, 2013) , grass carp (Lv, Hu, Xiong, You, & Fan, 2018) and so on. But there are few studies that have reported the mechanism which improved fish flesh quality by the depuration system treatment, thus further researches are still needed.

Metabolomics is the study of metabolites within organic tissues and biofluids to comprehensively identify and quantify all endogenous and exogenous low-molecular-weight

3

23 (<1000 *m/z*) molecules in a high-throughput manner, for observing the changes of the small

24 molecules with metabolic fingerprinting (changes of the metabolic patterns) or metabolic profiling

25 (changes of a group of metabolites or a specific pathway) due to endogenous and exogenous factors

26 (Feizi, Hashemi-Nasab, Golpelichi, Saburouh, & Parastar, 2021; Johnson, Sidwick, Pirgozliev, Edge,

27 & Thompson, 2019). Metabolomics has been extensively applied to food sciences with two major

28 aims, including the development of accurate and rapid food quality control methods and

29 investigation of nutritional effects of selected foods or food components (Gil, 2017). Non-targeted

30 metabolomics focus on finding as many small molecules as possible and global metabolic profiles,

31 so that they are particularly useful when differences between sample sets are very small, or finding

32 which compounds or classes of compounds are affected by the factor under investigation with

33 various detection technologies, such as nuclear magnetic resonance spectroscopy (NMR) (Labine

34 & Simpson, 2020), mass spectrometry (MS), *etc*. (Torres Santiago, Serrano Contreras, Meléndez

35 Camargo, & Zepeda Vallejo, 2019; Zhu et al., 2019). Among these different kinds of detection

36 technologies, the NMR-based method is a valuable tool for quantitatively identifying the different

37 metabolites in tissues, due to advantages, such as highly reproducible, minimal sample preparation

38 steps, nonrequirement   of standards and qualitative and quantitative measurement (Labine &

39 Simpson, 2020). Compared with the NMR-based method, the MS-based methods could offer higher

40 sensitivity than the NMR and also require much fewer samples (Sugimoto, Kawakami, Robert, Soga,

41 & Tomita, 2012). Currently, several types of MS techniques have been widely used in metabolomics

42 analysis, such as liquid chromatography-mass spectrometry (LC-MS) and gas chromatography–

43 mass spectrometry (GC-MS). Among these, LC-MS represented by UHPLC-Q-TOF-MS and

44 UHPLC-Q-Orbitrap HRMS dominates the metabolomics arena due to its high resolution and

45   sensitivity (Wang et al., 2014). Therefore, LC-MS based metabolomics fingerprinting approaches

46   have advantages on the evaluation of metabolic differences during various environmental systems

47   or feeding modes of aquatic products based on metabolic patterns and correlation with the alteration

48   of certain metabolic pathways (Cappello et al., 2016; Gika, Virgiliou, Theodoridis, Plumb, & Wilson,

49   2019; Zhang et al., 2019).

50   Transcriptomics is a high performance method used to study the differences which are implicit

51   in fish living in different environments at the mRNA level. Transcriptomics analysis can effectively

52   screen the differentially expressed genes (DEGs) of fish exposed to various environmental

53   pollutants (Zhang et al., 2019), pathogenic microbial invasion (Long et al., 2015), stress responses

54   (Petitjean et al., 2019) and their corresponding mechanisms. For example, short-term 17α -

55   ethynylestradiol exposure in sardine (*Sardinops sagax*) and mackerel (*Scomber japonicus*) disrupted

56   the basic biological processes and pathways and the corresponding diagnostic biomarkers that

57   monitor ocean environmental health were uncovered through transcriptomic analysis (Renaud et al.,

58   2019). Transcriptomics sequencing explores the mechanism of Grass carp reovirus infection, which

59   is involved in adsorption at the cell surface, followed by endocytosis into cells, transport of

60   lysosomes which eventually results in cell necrosis and/or apoptosis (Chen et al., 2018). A former

61   study (Sánchez et al., 2011) used transcriptomics to examine gene expression in different organs of

62   rainbow trout caused by temperature, salinity, crowding and hypoxia, a change of single nucleotide

63   polymorphism. The transcriptomic method has been applied to study the effects of long term

64   starvation and diet composition on the expression of mitochondrial oxidative phosphorylation gene

65   expression in gilthead sea bream (Silva-Marrero et al., 2017). In addition, transcriptomics can be

66   used to determine the ecological diversity, genetic diversity and evolution of fish (Hughes et al.,

67   2017; Sin-Yeon et al., 2017). Therefore, the application of transcriptomics to the analysis of genes

68   related to metabolic differences in the purification process of freshwater fish can clarify the

69   regulatory mechanism of the purification treatment that improves the quality of freshwater fish.

70   In the present study, metabolomics and transcriptomic responses in the flesh of market-size

71   crucian carp under treatment with short term micro-flowing purification system (STMFPS) were

72   investigated for up to 9 days and then the possible representative metabolites and different signal

73   pathways involved in the improvement of flesh quality for crucian carp were examined.

74

75   **2. Materials and Methods**

76   **2.1 Chemical reagents**

77   HPLC grade 2-Chloro-L-phenylalanine, methanol, acetonitrile and formic acid were obtained

78   from Sigma Aldrich (St. Louis, MO, USA). Biochemical reagent creatinine was purchased in

79   Biosharp (Hefei, Anhui, P.R. China). MS-222 (3-Aminobenzoic acid ethyl ester methanesulfonate)

80   was obtained from Shanghai Yuanye Bio-Technology Co., Ltd (Shanghai, P.R. China), which was

81   used to induce anesthesia in fresh crucian carp. The water used in all experiments was ultrapure

82   water from a Milli-Q system (Millipore, Billerica, MA, USA). All chemical reagents used and water

83   are chromatographic grade.

84   **2.2 Experimental design structure**

85   All animal standard operation procedures were approved by the Animal Care and Use

86   Committee of Huazhong Agricultural University and performed in accordance with the Guidelines

87   for Care and Use of Laboratory Animals of Huazhong Agricultural University. The whole

88   experimental design procedures are illustrated in Fig. 1. Briefly, the freshwater fish were obtained

89   from Honghu city (Hubei, P.R. China) and transferred to the short term micro-flowing water system.

90   The fish was depurated for different periods, and fresh muscle was obtained and extracted for the

91   metabolomics and transcriptomics studies. The detailed information is provided below.

92   **2.3 Fish sample preparation**

93   The fresh crucian carp (250~400 g) from the freshwater fish farming area in Honghu Deyan

94   Aquatic Product Company LTD were transported in troughs (Long × Width × Height: 7.0 m × 2.0

95   m × 0.8 m) with STMFPS. There were ~130 kg fish placed in each trough, the fish-water mass ratio

96   was 1:30, and the water was continuously replaced with groundwater as the source of water supply.

97   During the treatment period, the amount of water changed in each through was about 15.6 m^3/d,

98   around 400% (*v/v*), the temperature of water was 19.0±0.6 ℃, and all fish were deprived of food

99   during the whole period. During the period of depuration, five crucian carps of similar size were

100   randomly collected at every period of 0 d, 1 d, 5 d, 9 d. The sampled fish was anaesthetized using

101   the anesthetic MS－222 (100 mg/L) and was unconscious before slaughter. Fish were immediately

102   gutted and segmented. At the end, the dorsal muscle of each fish was taken and immediately frozen

103   with liquid nitrogen and stored at -80 °C for further analysis.

104   **2.4 Metabolites extraction and UPLC-QTOF-MS based metabolomics analysis**

105   The fish muscle samples (~50 mg) were extracted with methanol. Briefly, methanol (800 μL)

106   and the internal standard 2-chlorophenylalanine (2.8 mg/mL, 10 μL) were added to the sample. Then,

107   all fish samples were grinded for 90 s at 65 Hz, vortexed for 30 s and centrifuged for 15 min (12000

108   rpm, 4 °C).

109   The Acquity UPLC-QTOF system was used to separate and detect the metabolites of fish sample.

110   The UPLC system was equipped with a binary pump, micro degasser, an autosampler and a

temperature-controlled column compartment. Chromatographic separations were performed on an

ACQUITY UPLC HSS T3 column (1.8 μm, 2.1 mm × 100 mm; Waters, Ireland). 200 μL supernatant

was transferred to sample vials for UPLC-MS platform analysis, and compounds were eluted using

a binary phase at a flow rate of 0.35 mL/min, where solvent A was water containing 0.1% formic

acid (*v/v*) and solvent B was acetonitrile containing 0.1% formic acid (*v/v*). The following linear

gradient elution program was used: 0-2 min, 95% A; 2-12 min, 95–5% A; 12-15 min, 5% A; 15-17

min, 5–95% A; 17-20 min, 95% A. The column was maintained at 40 °C and the injection volume

was 0.6 μL. To avoid the effects of fluctuations in instrument detection signals, samples were

analyzed in random order. At the same time, quality control (QC) samples, which were prepared by

mixing all the samples, were inserted into the sample queue to monitor system stability and ensure

reliability of experimental data. The separated components were detected with a Xevo® G2-S QTof

mass spectrometer (Waters Corp., Mil-ford, MA, USA) operating in negative and positive

electrospray ionization (ESI) mode. Both ESI ion modes and conditions were collected as follows:

Cone gas, 50 L/h; Ion source temperature, 120 °C (+)/110 °C(−); Desolvation gas temperature,

350 °C; Capillary voltage, 1.4 kV(ESI+)/1.3 kV(ESI−); Sample cone, 40 V(ESI+) or 23 V(ESI−);

Gas flow, 600 L/h; Collision energy, 10–40 V; Ion energy: 1 V; Scan time: 0.03 s; Inter scan time:

0.2 s; Scan range 50–1500 m/z(Wang et al., 2019).

The raw data of UPLC-QTOF/MS were converted into *mz*ML format using ProteoWizard, and

XCMS was successively processed by peak alignment, peak detection, peak picking, peak filling,

isotope elimination, normalization and peak area extraction. Then, principal component analysis

(PCA) and orthogonal partial least squares discriminant analysis (OPLS-DA) of metabolome data

was performed in SIMCA-P 13.0 software (Umetrics AB, Umea, Sweden). With the data from both

ionization modes, the supervised multivariate data analysis approach OPLS-DA was used to screen

the significant different metabolites among the crucian carp samples in various purification periods.

A statistically explicit threshold based on the variable importance of projection (VIP) and the

student's *t*-tests (*p*-value) were used to identify metabolites with significant differences between the

control and STMFPS treated groups. The corresponding metabolic pathways analysis were

conducted using the MetaboAnalyst 4.0 software (http://www.metaboanalyst.ca/).

2.5 RNA extraction and transcriptomic analysis

To explore changes in mRNA levels of crucian carp after STMFPS treatment, fish samples (0

d, 1 d, 5 d, 9 d, n = 5 for every group) depurated in troughs were collected and used for RNA

extraction and RNA sequence analysis. The total RNA was isolated by TRIzol™ Reagent

(Invitrogen, Carlsbad, CA, USA) according to the manufacturer's protocol. The TruSeq RNA

sample preparation kit from Illumina (San Diego, CA, USA) was used for cDNA library preparation.

The cDNA library construction and sequencing and RNA-seq library preparation were performed

on an Agilent 2100 Bioanalyzer and ABI StepOnePlus™ Real-Time PCR System as described

previously (Trapnell et al., 2012). The obtained raw reads were cleaned by removing reads adapter

sequences, ploy-N strands and low-quality reads. High quality clean reads were used for

transcriptome *de novo* assembly using Trinity software (Wagner, Fulton, & Henschel, 2016). Clean

reads were aligned to carp (Cyprinus carpio) reference genome sequences by hierarchical indexing

for spliced alignment of transcripts with the application of HISAT2 (Kim, Langmead, & Salzberg,

2015). Gene expression was calculated using fragments per kilobase of exon per million mapped

reads (FRKM) approach. DESeq2 R package was utilized to illustrate the differential expressions

between the control group and treated groups (Varet, Brillet-Guéguen, Coppée, & Dillies, 2016).

155 Genes with an adjusted p-value < 0.05 obtained by DESeq2 were assigned as DEGs. Volcano plots

156 were drawn to exhibit the overall distribution of the DEGs in different treatment groups represented

157 by red, green and blue dots. These DEGs were then used to perform enrichment analysis of the Gene

158 Ontology (GO) (http:// www.geneontology.org/) and the Kyoto Encyclopedia of Genes and

159 Genomes (KEGG) pathway annotations. Each treatment had five biological replicates.

160 **2.6 Statistical analysis**

161 Statistical analysis was performed with SPSS 22.0 (IBM, New York, USA) using one-way

162 ANOVA. Significant differences between treatments were analyzed by Student's t-tests run in SPSS,

163 p-value < 0.05 was considered statistically significant. A statistical power analysis was used to

164 estimate the sample size for significant differences, which was implemented in freeware GPower

165 (Erdfelder, Faul, & Buchner, 1996), and metabolite network was constructed based in KEGG

166 pathways.

167

168 **3. Results and discussion**

169 **3.1 UPLC-QTOF/MS analysis**

170 To investigate the metabolite compositions during different purification periods, the non-

171 targeted metabolite profiling of extracts was detected. The flesh samples were collected from the

172 crucian carp under different purification periods (0 d, 1 d, 5 d and 9 d). The metabolites extracted

173 from muscles were screened with UPLC-QTOF/MS. In order to show differences in spectra among

174 different types of samples, a series of liquid chromatography are illustrated in Fig. S1A-S1D. Under

175 optimized elution conditions of ultra-high performance liquid chromatography, the elution periods

176 of the main period were around 0.9 min-3.6 min, 8.5 min-12.0 min, 13.0 min-16.5 min and ~18.0

177   min.

178   Based on *m/z* values and the standard libraries (METLIN, and HMDB – Human Metabolome

179   Database) by comparison, there were 342 metabolites (Putatively annotated compounds (Sumner et

180   al., 2007)) identified in the samples, including 71 amino acids and amino acid derivatives, 107 lipids,

181   52 nucleic acid hydrolysates and their derivatives, and 109 sugars and carbon sources chemicals. As

182   examples, a series of EIC (extracted ion chromatograms, Fig. S1E-S1H) and MS spectra (Fig. S1I-

183   S1L) were collected to show the steps of identification of metabolites, such as urea, pyruvate, retinol

184   and vitamin D3. It was very clear to see that there exists obvious differences among TIC

185   chromatograms from different types of samples. However, it was difficult to extract the potential

186   different metabolic markers in fish samples by intuitionally comparing the chromatograms from the

187   purified and control samples. Thus, the application of PCA and the pattern recognition method

188   (OPLS-DA) were used to visualize the characteristic changes.

189   **3.2 Principal component analysis**

190   To initially evaluate the differences among fish samples from different purification periods, a

191   non-supervised multivariate analysis method, PCA was used to analyze the multidimensional data

192   and provide a comprehensive view of the clustering among different samples.

193   The UPLC-QTOF/MS data under ES+ mode was first utilized to conduct an overview of the

194   clustering models and search possible outliers among samples. After reducing dimensions of the

195   metabolic data matrix by dropping unnecessary information, the first two principal components PC1

196   and PC2 were obtained for these four different groups. The total contribution of the first two major

197   components was 49.2% of the variance for all variables, and the scatter plot for PC1 (34.4%) and

198   PC2 (14.8%) is illustrated in Fig. 2A. It clearly can be seen that fish samples were clustered together

199 after five or nine days' purification. The one-day purification treatment also influenced the

200 components of the samples, as the samples were disperse distributed in the 2D space, one sample

201 was out of space, and the samples were not clustered with samples in the control group. Then, the

202 PCA models of 0 d *vs.* 1 d, 0 d *vs.* 5 d, and 0 d *vs.* 9 d were further conducted and illustrated in Fig.

203 2B (PC1: 30.4%; PC2: 21.1%), 2C (PC1: 53.1%; PC2: 13.9%) and 2D (PC1: 43.4%; PC2: 17.1%),

204 respectively. The results are similar to the findings in Fig. 2A. The statistical parameters (R^2 and Q^2)

205 of all PCA models are collected in Table 1. To screen the different metabolites among the control

206 and treatment groups with short-term purification periods, the different metabolites were further

207 explored with OPLS-DA methods.

3.3 OPLS-DA analysis

209   The OPLS-DA models were achieved by making comparisons between 0 d *vs.* 1 d; 0 d *vs.* 5 d

210 and 0 d *vs.* 9 d. The evaluation parameters of these models (R^2Y and Q^2) are demonstrated in Table

211 1. The permutation test plots from the OPLS-DA models based on the positive ion mode are

212 illustrated in Fig. 2E-2G. The models for comparisons of 0 d *vs.* 5 d and 0 d *vs.* 9 d under positive

213 and negative ion mode data showed that the classification models were stable and reliable (R^2 and

214 $Q^2{\geq}0.5$). The values of R^2Y sufficiently explained the differences between these two groups and the

215 values of Q^2 indicate the predictive abilities of the constructed classification models. Furthermore,

216 the models for comparisons of 0 d *vs.* 1 d under different ion modes explained the differences

217 between these two groups ($R^2Y>0.9$), but there was over-fitting in the negative ion mode ($Q^2<0.5$).

3.4 Identification of different metabolites of crucian carp during STMFPS treatment

219   The different metabolic patterns between every comparison were recognized according to their

220 VIP > 1.5 and $p < 0.05$ values. Finally, the metabolic numbers for these three different comparisons

221 (0d vs. 1d, 0d vs. 5d and 0d vs. 9d) were 22, 81 and 64 of various metabolites, respectively. To

222 analyze the efficiency of the short-term purification treatment, the different metabolites under two

223 different periods were annotated.

224 To further identify the biomarkers at different short-term purification periods, the different

225 metabolites and their relative contents among different groups were identified and analyzed. The

226 selected metabolites were identified using m/z information of the metabolites and the Tandem MS

227 database (METLIN and HMDB) and KEGG database. The identified results are shown in Table 2.

228 Results of the statistical power were also calculated and displayed in this table, which was used to

229 estimate the sample size to determine the significant difference (*: ≥ 0.8 for sufficient power

230 validation). Finally, there were 10 metabolites which changed during the whole purification period;

231 and 31 metabolites changed in two different treatment periods (Table 2). Changes can be seen in the

232 types and contents of different metabolites of crucian carp muscles under different treatment periods.

233 The metabolic pathways that underwent significant changes during microfluidic treatment

234 mainly include TCA cycle, ornithine cycle, purine metabolism and amino acid catabolism. Among

235 them, the metabolic changes related to the TCA cycle mainly showed that pyruvate, succinic acid,

236 and coenzyme $Q2$ significantly decreased on days 5 and 9 after purification (as shown in Fig. 3A-

237 3C) and AMP (Adenosine monophosphate) significantly increased after purification (Fig. 3D). The

238 purine metabolism changes mainly indicated that the content of guanosine, guanine, and adenine

239 increased significantly after 5 days' treatment (Fig. 3E-3G) and the content of ornithine, a product

240 of purine catabolism, decreased significantly after 5 days of treatment (Fig. 3H). The difference in

241 ornithine cycle metabolism is mainly due to the accumulation of oxalic acid and arginine succinic

242 acid (Fig. 3I-3J) and the significant reduction in citrulline content after 5 days of microfluidic

13

243　treatment (Fig. 3K). The difference in amino acid metabolism is mainly manifested as changes in

244　the content of free amino acids such as proline, tyrosine, tryptophan, and lysine after microfluidic

245　treatment. Among them, the contents of serine and tyrosine increased after treatment, while the

246　contents of tryptophan and lysine decreased. At the same time, a large amount of

247　monoacylphospholipid molecules were observed during the microfluidic treatment process,

248　indicating that the carp muscle phospholipid metabolism was active during the treatment process.

249　　Due to changes in metabolites and the reported pathway of the metabolites in the KEGG

250　database, the changes of the metabolic pathway of the crucian carp muscle during the short-term

251　purification periods were obtained (Fig. 4). After the crucian carp was transferred from the

252　aquaculture/transportation water to the STMFPS purified water, the ornithine cycle metabolism

253　related to ammonia nitrogen excretion changed, at the same time, due to lack of food, the TCA cycle

254　in the muscles of crucian carp weakened, causing changes in amino acid metabolism and purine

255　metabolism to compensate for the required energy that maintain normal life activities. During this

256　process, ornithine, arginine succinic acid and some purine nucleosides and purine bases accumulated

257　affecting the flesh quality of crucian carp.

258　**3.5 Metabolic mechanism of STMFPS to improve the flesh quality of crucian carp**

259　　Changes in differential metabolites of crucian carp indicate that the ornithine cycle metabolic

260　pathway underwent significant changes during STMFPS treatment. Generally, seven key enzymes

261　including carbamyl phosphate synthetase (CPS-1), ornithine carbamoyltransferase (OTC), spermine

262　succinate synthetase (argininosuccinate synthetase, ASS), argininosuccinate lyase (ASL), arginase

263　(arginase), N-acetyl glutamate synthetase (N- acetylglutamate synthetase) and ornithine

264　aminotransferase (OAT) are involved in ornithine cycle metabolism in the animal body and

265 responsible for the synthesis of related substrates and related transport proteins for transmembrane

266 transport (Morris, 2002).

267 When the crucian carp was transferred to clean water for a short period of treatment, with

268 changes in ammonia nitrogen concentration gradient in the environment, the direct excretion of

269 ammonia was inhibited and the activity of urea cycle-related enzymes and the synthesis of ornithine

270 to citrulline rose, including CPS-1 in the liver and synthesis of arginine succinic acid in the liver

271 and arginine succinate lyase (Saha & Ratha, 2007). Thus, the content of citrulline in muscle was

272 significantly reduced, while the content of ornithine and arginine succinic acid increased. Ornithine

273 in the body may also derive from the metabolism of glutamate and glutamine (Blachier, Boutry, Bos,

274 & Tomé, 2009), and the synthesis and accumulation of glutamine is one of the defense mechanisms

275 of freshwater fish against a high ammonia nitrogen environment. A study reported a similar finding

276 that glutamine may accumulate in many tissues of crucian carp during the cultivation or

277 transportation process (Zhang, Zhang, Wang, Gu, & Fan, 2017). As blood ammonia nitrogen levels

278 decrease in STMFPS, glutamine produces ornithine under the action of glutaminase and P5C

279 synthetase, which may be one of the major reasons for the increase in ornithine content in crucian

280 carp flesh. Ornithine is an important flavor precursor and its derivative 1-pyrroline is one of the

281 important substrates for Maillard reaction (Corral, Leitner, Siegmund, & Flores, 2016). Furthermore,

282 ornithine can also reduce the bitterness of other amino acids in the food system to improve the flavor

283 of food (Wan, Xiong, Zhang, & Zhu, 2013). Therefore, the accumulation of ornithine could be

284 responsible for the enhancement of the crucian carp flavor during the STMFPS treatment.

285 **3.6 Transcriptomics profiling and DEGs**

286 The RNA-seq results indicate that the total number of genes expressed were distinct in the

287 control group and STMFPS-treated groups. In order to reflect the correlation of gene expression

288 between the samples, the Pearson correlation coefficient of all gene expression levels between each

289 of two different experimental groups was calculated. The correlation between the detected gene

290 expression profiles of STMFPS-treated groups and control groups are presented in Fig. 5. The

291 correlation is better when the correlation coefficient is closer to 1.00. Therefore, this figure could

292 directly display the significant difference between the different treatment groups making the

293 grouping clear. From Fig. 5, it can be seen that the correlation of samples between 0 d (control group)

294 and 1 d was high ($p>0.975$), indicating that the expression levels of different genes or

295 transcriptomics profiling in the crucian carp muscles were similar. The correlation coefficients

296 between the samples STMFPS-treated at 0 d and 5 d, 0 d and 9 d were low, demonstrating that the

297 expression levels of various genes in crucian carp samples greatly changed after 5 d and 9 d

298 STMFPS treatment.

299 Comparing with the control group, the DEGs were identified with the following statistical values

300 for the genes: $p < 0.05$ and |log2FC (fold change) | ≥ 2. The number of DEGs which overlapped

301 between different STMFPS-treated periods and control groups are shown in the Venn diagram (Fig.

302 6A). Finally, there were 5917, 15085, 14183 DEGs identified between the 1 d, 5 d, 9 d STMFPS

303 treated group and the control group (Ctr), and 3246 identical genes were found for these three

304 different comparisons. The MA plots were drawn to intuitively represent the DEGs distribution or

305 the degree of variation of these DEGs between different STMFPS treated and control groups (Fig.

306 6B). The abscissa represents A value (Average log CPM, log2 (counts -per-million)) used to measure

307 the amount of gene expression. Vertical axis represents the M value (log2FC) used to estimate the

308 up- and down-regulation of gene expression. The red dots indicate the upregulated expressed genes

309   (|log2FC (fold change)|≥ 2, q ≤ 0.001), the blue dots represent the downregulated expressed genes

310   (Log2FC(fold change) ≤ -2, q ≤ 0.001), and the grey dots, the nondifferential expressed genes (abs

311   (Log2FC(fold change)) ≤ 2, q > 0.001). As it can be seen from Fig. 6B, compared with the untreated

312   samples, most of DEGs in the crucian carp muscle samples after STMFPS treatment were up-

313   regulated and the number of up-regulated genes elevated to the highest level at 5 d STMFPS

314   treatment. The M values of most DEGs are distributed in -4 ~ 3, -4 ~ 6 and -4 ~ 5 between the

315   control groups versus 1 d, 5 d and 9 d STMFPS treated groups. The number of DEGs increased with

316   the range of M values, so the number of DEGs between Ctr *vs.* Day5 was the largest during the

317   STMFPS treatment. Results of transcriptomic analysis indicate that the STMFPS treatment affected

318   the expression of many genes in the crucian carp muscle. Compared with the control group, there

319   were 4776, 14174, 13211 upregulated genes and 1141, 911, 972 downregulated genes found for

320   different STMFPS-treated groups (1 d, 5 d, 9 d), respectively.

321   The expression levels of genes of all samples (control, 1 d, 5 d and 9 d) were produced with five

322   biological replicates per treatment and are shown in the clustered heatmap (Fig. 6C). The gene

323   expression status of crucian carp muscles under different purification periods was mainly divided

324   into two parts, the gene expression of crucian carp samples treated on 0 d and 1 d is very similar

325   and the transcription profiling of crucian carp samples treated on 5 d and 9 d by STMFPS bear a

326   resemblance. Furthermore, there exist a big difference between 5 d/9 d STMFPS treated crucian

327   carp samples and 0 d/1 d samples in gene expression levels. Basically, the transcriptome profiles of

328   three STMFPS treatment groups were different compared with the control group.

329   **3.7 GO enrichment analyses of DEGs**

330   The classification and enrichment of DEGs help us to understand the functional properties of

331 DEGs detected in crucian carp muscle samples during different STMFPS treatment periods.

332 Generally, gene ontology (GO) can be classified into three functional categories, including the

333 molecular function, cellular component and biological process (Chen et al., 2018). Results of the

334 GO function classification of DEGs under different treatment periods are plotted in Fig. 7. It can be

335 seen that the cellular process, single-organism process and metabolic process are the top three

336 functional classes of DEGs during the STMFPS treatment. For the metabolic process, there were

337 1322, 3299, 3026 DEGs identified between the control and the other three different STMFPS

338 treatment groups (1 d, 5 d and 9 d), respectively. Furthermore, it can clearly be noticed that the

339 number of DEG in crucian carp flesh is affected by the period of STMFPS treatment. Moreover, the

340 number of DEGs involved in the metabolic process in crucian carp flesh reached a maximum at 5 d

341 STMFPS treatment, and then it tended to stabilize after 9 d STMFPS treatment.

342 **3.8 KEGG Metabolic Pathway analysis of DEGs**

343 In order to compare the transcriptome and metabolome data, the metabolic pathways of DEGs

344 involved in the KEGG database were further analyzed. The detailed metabolic pathway and the

345 corresponding number of DEGs of each metabolic pathway are listed in Table 3. As can be seen,

346 purine metabolism, pyrimidine metabolism and glycerophospholipid metabolism represent the

347 majority of metabolic pathways, which take up the top three number of DEGs between the control

348 group and the other three STMFPS treatments groups. It means that STMFPS treatment mainly

349 resulted in changes in nucleotide and phospholipid metabolism in the muscle of crucian carp flesh.

350 Transcriptomics analysis indicates that STMFPS treatment can affect the purine metabolism of

351 freshwater fish, which induced the accumulation of single nucleotides IMP and AMP in crucian carp

352 flesh, reduced the content of xanthine, hypoxanthine and other single nucleotide degradation

353   products, thus affecting the flesh quality of freshwater fish. Therefore, the results of transcriptomics

354   were in good accord with the results of metabolomics of crucian carp treated with STMFPS.

355   According to the results of DEGs in the metabolic classification, combined with the ornithine

356   cycle-related metabolic pathways in the KEGG database, the expression of ornithine cycle-related

357   genes was analyzed. The DEGs are shown in Table 4. It can be seen that the STMFPS treatment led

358   to differential expression of seven enzyme genes related to the ornithine cycle in the flesh of crucian

359   carp. Among these, the ornithine oxoaminotransferase gene was down-regulated and the other

360   enzyme genes were up-regulated. The expressions of arginine succinate synthetase and arginine

361   succinate lyase were up-regulated, which is in accordance with results of the metabolomics study,

362   in other words, STMFPS induced citrulline and metabolized more arginine succinate in freshwater

363   fish flesh. Furthermore, the upregulated genes of enzymes including N-alpha-acetyltransferase,

364   pyrroline-5-carboxylate reductase, delta-1-pyrroline-5-carboxylate synthetase and carbamoyl-

365   phosphate synthase were intermediate catalytic enzyme genes for the synthesis of ornithine by

366   glutamic acid and proline, respectively. Therefore, the results of DEGs related to the ornithine cycle

367   in this study support the results of changes in the content of related metabolites. In this regard,

368   STMFPS treatment affected the ornithine cycle metabolic pathways in freshwater fish and led the

369   content of ornithine and spermine aminosuccinic acid to increase significantly, however the contents

370   of citrulline, proline, urea decreased significantly, thereby affecting the flesh quality of crucian carp.

371

372   **4. Conclusion**

373   In summary, the current integrative application of transcriptome and metabolome approaches

374   has potential implications for understanding the effect of flesh quality improvement with STMFPS

375 treatment. UPLC-QTOF MS based metabolomics showed that STMFPS affected TCA cycle,

376 ornithine cycle, purine metabolism, amino acid metabolism and fatty acid metabolism pathways in

377 crucian carp flesh. Results of transcriptome were basically in agreement with the metabolome and

378 to explore insights to understanding the flesh quality improvement of market size crucian carp,

379 STMFPS treatment was used. Transcriptome showed that STMFPS treatment induced significant

380 changes in various genes involved in purine and arginine metabolism pathways. These results

381 provided some information for understanding the main metabolic mechanism for improving the

382 flesh quality of crucian carp of STMFPS treatment.

383

384 **Credit authorship contribution statement**

385 **Hongying Du**: Investigation, Writing - original draft and review, Formal analysis, Visualization,

386 Conceptualization, Funding acquisition; **Shanbai Xiong**: Funding acquisition, Supervision,

387 Conceptualization; **Hao Lv**: Investigation, Formal analysis, Validation, Methodology; **Siming Zhao**:

388 Investigation; **Anne Manyande**: Writing - review & editing.

389

390 **Conflict of interest**

391 The authors declare that there is no conflict of interest

392

398

399   **References**

400   Blachier, F., Boutry, C., Bos, C., & Tomé, D. (2009). Metabolism and functions of l-glutamate in the
401   epithelial cells of the small and large intestines. *The American Journal of Clinical Nutrition,*
402   *90*(3), 814S-821S. doi: https://doi.org/10.3945/ajcn.2009.27462S

403   Burr, G. S., Wolters, W. R., Schrader, K. K., & Summerfelt, S. T. (2012). Impact of depuration of
404   earthy-musty off-flavors on fillet quality of Atlantic salmon, Salmo salar, cultured in a
405   recirculating aquaculture system. *Aquacultural Engineering, 50*, 28-36. doi:
406   https://doi.org/10.1016/j.aquaeng.2012.03.002

407   Cappello, T., Brandão, F., Guilherme, S., Santos, M. A., Maisano, M., Mauceri, A., . . . Pereira, P.
408   (2016). Insights into the mechanisms underlying mercury-induced oxidative stress in gills
409   of wild fish (Liza aurata) combining 1H NMR metabolomics and conventional biochemical
410   assays. *Science of The Total Environment, 548-549*, 13-24. doi:
411   https://doi.org/10.1016/j.scitotenv.2016.01.008

412   Chen, G., He, L., Luo, L., Huang, R., Liao, L., Li, Y., . . . Wang, Y. (2018). Transcriptomics Sequencing
413   Provides Insights into Understanding the Mechanism of Grass Carp Reovirus Infection.
414   *International Journal of Molecular Sciences, 19*(2), 488-498. doi:
415   https://doi.org/10.3390/ijms19020488

416   Corral, S., Leitner, E., Siegmund, B., & Flores, M. (2016). Determination of sulfur and nitrogen
417   compounds during the processing of dry fermented sausages and their relation to amino
418   acid generation. *Food Chemistry, 190*, 657-664. doi:
419   https://doi.org/10.1016/j.foodchem.2015.06.009

420   Cui, D., Zhang, P., Li, H., Zhang, Z., Luo, W., & Yang, Z. (2020). Biotransformation of dietary
421   inorganic arsenic in a freshwater fish Carassius auratus and the unique association
422   between arsenic dimethylation and oxidative damage. *Journal of Hazardous Materials,*
423   *391*, 122153. doi: https://doi.org/10.1016/j.jhazmat.2020.122153

424   Drake, S. L., DRAKE, M. A., Sanderson, R., Daniels, H. V., & Yates, M. D. (2010). The effect of purging
425   time on the sensory properties of aquacultured southern flounder (paralichthys
426   lethostigma). *Journal of Sensory Studies, 25*(2), 246-259. doi:
427   https://doi.org/10.1111/j.1745-459X.2009.00255.x

428   Erdfelder, E., Faul, F., & Buchner, A. (1996). GPOWER: A general power analysis program. *Behavior*
429   *Research Methods, Instruments, & Computers, 28*(1), 1-11. doi:
430   https://doi.org/10.3758/BF03203630

431   Feizi, N., Hashemi-Nasab, F. S., Golpelichi, F., Saburouh, N., & Parastar, H. (2021). Recent trends in
432   application of chemometric methods for GC-MS and GC×GC-MS-based metabolomic
433   studies. *TrAC Trends in Analytical Chemistry, 138*, 116239. doi:
434   https://doi.org/10.1016/j.trac.2021.116239

435   Fuentes, A., Fernández-Segovia, I., Serra, J. A., & Barat, J. M. (2010). Comparison of wild and
436   cultured sea bass (Dicentrarchus labrax) quality. *Food Chemistry, 119*(4), 1514-1518. doi:
437   https://doi.org/10.1016/j.foodchem.2009.09.036

438 Gika, H., Virgiliou, C., Theodoridis, G., Plumb, R. S., & Wilson, I. D. (2019). Untargeted LC-MS-based
439   metabolic phenotyping (metabonomics/metabolomics): The state of the art. *Journal of*
440   *Chromatography B, 1117*, 136-147. doi: https://doi.org/10.1016/j.jchromb.2019.04.009
441 Gil, A. M. (2017). Metabonomics in Food Science. In J. C. Lindon, G. E. Tranter & D. W. Koppenaal
442   (Eds.), *Encyclopedia of Spectroscopy and Spectrometry (Third Edition)* (pp. 790-796).
443   Oxford: Academic Press.
444 Grigorakis, K., Taylor, K. D. A., & Alexis, M. N. (2003). Organoleptic and volatile aroma compounds
445   comparison of wild and cultured gilthead sea bream (Sparus aurata): sensory differences
446   and possible chemical basis. *Aquaculture, 225*(1), 109-119. doi:
447   https://doi.org/10.1016/S0044-8486(03)00283-7
448 Hughes, L. C., Somoza, G. M., Nguyen, B. N., Bernot, J. P., González-Castro, M., Díaz de Astarloa,
449   J. M., & Ortí, G. (2017). Transcriptomic differentiation underlying marine-to-freshwater
450   transitions in the South American silversides Odontesthes argentinensis and
451   O. bonariensis (Atheriniformes). *Ecology and evolution, 7*(14), 5258-5268. doi:
452   https://doi.org/10.1002/ece3.3133
453 Johnson, A. E., Sidwick, K. L., Pirgozliev, V. R., Edge, A., & Thompson, D. F. (2019). The use of
454   metabonomics to uncover differences between the small molecule profiles of eggs from
455   cage and barn housing systems. *Food Control, 100*, 165-170. doi:
456   https://doi.org/10.1016/j.foodcont.2019.01.023
457 Kim, D., Langmead, B., & Salzberg, S. L. (2015). HISAT: a fast spliced aligner with low memory
458   requirements. *Nature Methods, 12*(4), 357-360. doi: https://doi.org/10.1038/nmeth.3317
459 Labine, L. M., & Simpson, M. J. (2020). The use of nuclear magnetic resonance (NMR) and mass
460   spectrometry (MS)–based metabolomics in environmental exposure assessment. *Current*
461   *Opinion in Environmental Science & Health, 15*, 7-15. doi:
462   https://doi.org/10.1016/j.coesh.2020.01.008
463 Ling, X.-d., Dong, W.-t., Zhang, Y., Qian, X., Zhang, W.-d., He, W.-h., . . . Liu, J.-x. (2019).
464   Comparative transcriptomics and histopathological analysis of crucian carp infection by
465   atypical Aeromonas salmonicida. *Fish & Shellfish Immunology, 94*, 294-307. doi:
466   https://doi.org/10.1016/j.fsi.2019.09.006
467 Long, M., Zhao, J., Li, T., Tafalla, C., Zhang, Q., Wang, X., . . . Li, A. (2015). Transcriptomic and
468   proteomic analyses of splenic immune mechanisms of rainbow trout (Oncorhynchus
469   mykiss) infected by Aeromonas salmonicida subsp. salmonicida. *Journal of Proteomics,*
470   *122*, 41-54. doi: https://doi.org/10.1016/j.jprot.2015.03.031
471 Lv, H., Hu, W., Xiong, S., You, J., & Fan, Q. (2018). Depuration and starvation improves flesh quality
472   of grass carp (Ctenopharyngodon idella). *Aquaculture Research, 49*(9), 3196-3206. doi:
473   https://doi.org/10.1111/are.13784
474 Morris, S. M. (2002). Regulation of enzymes of the urea cycle and arginine metabolism. *Annual*
475   *Review of Nutrition, 22*(1), 87-105. doi:
476   https://doi.org/10.1146/annurev.nutr.22.110801.140547
477 Petitjean, Q., Jean, S., Gandar, A., Côte, J., Laffaille, P., & Jacquin, L. (2019). Stress responses in fish:
478   From molecular to evolutionary processes. *Science of The Total Environment, 684*, 371-
479   380. doi: https://doi.org/10.1016/j.scitotenv.2019.05.357
480 Renaud, L., Agarwal, N., Richards, D. J., Falcinelli, S., Hazard, E. S., Carnevali, O., . . . Hardiman, G.
481   (2019). Transcriptomic analysis of short-term 17α-ethynylestradiol exposure in two

482   Californian sentinel fish species sardine (Sardinops sagax) and mackerel (Scomber
483   japonicus). *Environmental Pollution, 244*, 926-937. doi:
484   https://doi.org/10.1016/j.envpol.2018.10.058

485 Rincón, L., Castro, P. L., Álvarez, B., Hernández, M. D., Álvarez, A., Claret, A., . . . Ginés, R. (2016).
486   Differences in proximal and fatty acid profiles, sensory characteristics, texture, colour and
487   muscle cellularity between wild and farmed blackspot seabream (Pagellus bogaraveo).
488   *Aquaculture, 451*, 195-204. doi: https://doi.org/10.1016/j.aquaculture.2015.09.016

489 Sánchez, C. C., Weber, G. M., Gao, G., Cleveland, B. M., Yao, J., & Rexroad, C. E. (2011). Generation
490   of a reference transcriptome for evaluating rainbow trout responses to various stressors.
491   *BMC Genomics, 12*(1), 626-636. doi: https://doi.org/10.1186/1471-2164-12-626

492 Saha, N., & Ratha, B. K. (2007). Functional ureogenesis and adaptation to ammonia metabolism in
493   Indian freshwater air-breathing catfishes. *Fish Physiology & Biochemistry, 33*(4), 283-295.
494   doi: https://doi.org/10.1007/s10695-007-9172-3

495 Schrader, K. K., Davidson, J. W., & Summerfelt, S. T. (2013). Evaluation of the impact of nitrate-
496   nitrogen levels in recirculating aquaculture systems on concentrations of the off-flavor
497   compounds geosmin and 2-methylisoborneol in water and rainbow trout (Oncorhynchus
498   mykiss). *Aquacultural Engineering, 57*, 126-130. doi:
499   https://doi.org/10.1016/j.aquaeng.2013.07.002

500 Silva-Marrero, J. I., Sáez, A., Caballero-Solares, A., Viegas, I., Almajano, M. P., Fernández, F., . . .
501   Metón, I. (2017). A transcriptomic approach to study the effect of long-term starvation
502   and diet composition on the expression of mitochondrial oxidative phosphorylation genes
503   in gilthead sea bream (Sparus aurata). *BMC Genomics, 18*(1), 768-779. doi:
504   https://doi.org/10.1186/s12864-017-4148-x

505 Sin-Yeon, Kim, Maria, M., Costa, Anna, . . . Velando. (2017). Transcriptional mechanisms underlying
506   life-history responses to climate change in the three-spined stickleback. *Evolutionary*
507   *Applications, 10*, 718-730. doi: https://doi.org/10.1111/eva.12487

508 Su, J., Luo, Y., Jiao, X., & Wu, J. (2017). Effect of the ecological fish farming technique on the muscle
509   quality of crucian carp (*Carassius auratus*). *Journal of Aquaculture, 38*(4), 22-25.

510 Sugimoto, M., Kawakami, M., Robert, M., Soga, T., & Tomita, M. (2012). Bioinformatics Tools for
511   Mass Spectroscopy-Based Metabolomic Data Processing and Analysis. *Current*
512   *Bioinformatics, 7*(1), 96-108. doi: Doi 10.2174/157489312799304431

513 Sumner, L. W., Amberg, A., Barrett, D., Beale, M. H., Beger, R., Daykin, C. A., . . . Viant, M. R. (2007).
514   Proposed minimum reporting standards for chemical analysis. *Metabolomics, 3*(3), 211-
515   221. doi: 10.1007/s11306-007-0082-2

516 Torres Santiago, G., Serrano Contreras, J. I., Meléndez Camargo, M. E., & Zepeda Vallejo, L. G.
517   (2019). NMR-based metabonomic approach reveals changes in the urinary and fecal
518   metabolome caused by resveratrol. *Journal of Pharmaceutical and Biomedical Analysis,*
519   *162*, 234-241. doi: https://doi.org/10.1016/j.jpba.2018.09.025

520 Trapnell, C., Roberts, A., Goff, L., Pertea, G., Kim, D., Kelley, D. R., . . . Pachter, L. (2012). Differential
521   gene and transcript expression analysis of RNA-seq experiments with TopHat and
522   Cufflinks. *Nature Protocols, 7*(3), 562-578. doi: https://doi.org/10.1038/nprot.2012.016

523 Varet, H., Brillet-Guéguen, L., Coppée, J. Y., & Dillies, M. A. (2016). SARTools: A DESeq2- and
524   EdgeR-Based R Pipeline for Comprehensive Differential Analysis of RNA-Seq Data. *Plos*
525   *One, 11*, e0157022. doi: https://doi.org/10.1371/journal.pone.0157022

526 Wagner, M., Fulton, B., & Henschel, R. (2016). *Performance Optimization for the Trinity RNA-Seq*
527   *Assembler*, Cham, 29-40.
528 Wan, H., Xiong, Y., Zhang, J., & Zhu, C. (2013). Research progress in products exploitation and
529   application of L-ornithine. *China Brewing, 32*, 8-12. doi: https://doi.org/0254-
530   5071(2013)01-0008-05
531 Wang, H., Li, S., Qi, L., Xu, W., Zeng, Y., Hou, Y., . . . Sun, C. (2014). Metabonomic analysis of
532   quercetin against the toxicity of chronic exposure to low-level dichlorvos in rats via ultra-
533   performance liquid chromatography–mass spectrometry. *Toxicology Letters, 225*(2), 230-
534   239. doi: https://doi.org/10.1016/j.toxlet.2013.12.017
535 Wang, Y., Li, C., Li, L., Yang, X., Chen, S., Wu, Y., . . . Yang, D. (2019). Application of UHPLC-Q/TOF-
536   MS-based metabolomics in the evaluation of metabolites and taste quality of Chinese fish
537   sauce (Yu-lu) during fermentation. *Food Chemistry, 296*(OCT.30), 132-141. doi:
538   https://doi.org/10.1016/j.foodchem.2019.05.043
539 Wu, S. (2020). Dietary Astragalus membranaceus polysaccharide ameliorates the growth
540   performance and innate immunity of juvenile crucian carp (Carassius auratus).
541   *International Journal of Biological Macromolecules, 149*, 877-881. doi:
542   https://doi.org/10.1016/j.ijbiomac.2020.02.005
543 Zajic, T., Mraz, J., Sampels, S., & Pickova, J. (2013). Fillet quality changes as a result of purging of
544   common carp (Cyprinus carpio L.) with special regard to weight loss and lipid profile.
545   *Aquaculture, 400-401*, 111-119. doi: https://doi.org/10.1016/j.aquaculture.2013.03.004
546 Zhang, W., Tan, B., Ye, G., Wang, J., Dong, X., Yang, Q., . . . Zhang, H. (2019). Identification of
547   potential biomarkers for soybean meal-induced enteritis in juvenile pearl gentian grouper,
548   Epinephelus lanceolatus ♂ × Epinephelus fuscoguttatus ♀. *Aquaculture, 512*, 734337. doi:
549   https://doi.org/10.1016/j.aquaculture.2019.734337
550 Zhang, Y., Zhang, H., Wang, L., Gu, B., & Fan, Q. (2017). Impact factors of ammonia toxicity and
551   strategies for ammonia tolerance in air-breathing fish: A review. *Acta Hydrobiologica*
552   *Sinica, 41*(5), 1157-1167. doi: https://doi.org/10.7541/2017.144
553 Zhu, H., Wang, Z., Wu, Y., Jiang, H., Zhou, F., Xie, X., . . . Hua, C. (2019). Untargeted metabonomics
554   reveals intervention effects of chicory polysaccharide in a rat model of non-alcoholic fatty
555   liver disease. *International Journal of Biological Macromolecules, 128*, 363-375. doi:
556   https://doi.org/10.1016/j.ijbiomac.2019.01.141
557
558

559 Figure legends**:**

560 **Fig. 1** Flow diagram of the experimental design.

561 **Fig. 2** Results of PCA analysis (A-D) and the permutation test plots (E-G) from the OPLS-DA

562   models for the metabolites detected using UPLC-QTOF/MS equipped with both ESI+ mod

563   which were obtained from crucian carp muscle during different depuration periods. *Note: A:*

564   *All samples in four groups; B: Control vs. 1 d; C: Control vs. 5 d; D: Control vs. 9 d; E:*

565   *Control vs. 1 d; F: Control vs. 5 d; G: Control vs. 9 d. The criteria for validity of the OPLS-*

566   *DA model are indicated as following: All blue Q^2-values to the left are lower than the*

567   *original points to the right; or the blue regression line of the Q^2-pints intersected the vertical*

568   *axis (on the left) or below zero.*

569 **Fig. 3**: Comparative contents of different metabolites in crucian carp muscle during the depuration

570   procedure ("*": <0.05; "**": $p<0.01$; "***": $p<0.001$). Note: A-D: Related with energy

571   metabolism; E-H: Related with the purine metabolic cycle; I-K: Related with the ornithine

572   metabolic cycle.

573 **Fig. 4** Effect of the depuration on metabolic pathways of crucian carp muscle. Note: *Different*

574   *colors of metabolites represent change of comparative content, red: increased; blue: did not*

575   *significantly change; green: decreased.*

576 **Fig. 5** Correlation heatmap of the Pearson correlation coefficient of all gene expressions in four

577   different groups (Ctr1-Ctr5: Control; Day1: 1 d; Day5: 5 d; Day9: 9 d).

578 **Fig. 6** (A) Venn diagram of significantly enriched DEGs in different group comparisons representing

579   the unique and overlapping DEGs. (B) MA plot distribution of DEGs of crucian carp muscle

580   during different deputation periods. The red and blue dots indicate that the genes were

581   differently expressed, and the grey dots indicate that the genes were not differentially expressed.

582   The positive and negative values represent the up- and downregulation of DEGs, respectively.

583   (C) Clustered heatmap for DEGs detected from different groups with rows representing DEGs

584   and columns representing samples. *Note: Columns represent every gene set that was*

585   *significantly up-regulated (red) or down-regulated (blue) in different groups (Ctr1-Ctr5:*

586   *Control; Day1: 1 d; Day5: 5 d; Day9: 9 d).*

587 Fig. 7 GO classification of DEGs. (A) GO functional classification of DEGs between control (Ctr)

588   and Day1. (B) GO functional classification of DEGs between Ctr and Day5. (C) GO functional

589   classification of DEGs between Ctr and Day9. (Ctr, Day1, Day5, Day9 represent 0 d, 1 d, 5 d

590   and 9 d STMFPS treatment groups, respectively).

591

592 Table 1: Collection of parameters of PCA and OPLS-DA models for the comparisons of

593 metabolites in crucian carp muscle treated at different depuration periods

Ions modes	Comparisons	PCA		OPLS-DA		
		R^2X	Q^2	R^2X	R^2Y	Q^2
ESI+	A vs. B	0.705	0.112	0.386	0.944	0.648
	A vs. C	0.670	0.351	0.658	0.999	0.983
	A vs. D	0.611	0.341	0.543	0.999	0.972
ESI-	A vs. B	0.584	-0.00327	0.238	0.997	0.287
	A vs. C	0.621	0.349	0.691	0.998	0.915
	A vs. D	0.547	0.234	0.494	0.998	0.961

594 （Note: A、B、C、D represents the different groups treated at different depuration periods, such as 0 d、1 d、5

595 d、9 d）

596

597

Table 2: Collection of different metabolites in crucian carp muscle during different depuration periods. *Note, Data was calculated as the ratio of the relative concentrations of the metabolites between depurated samples and the control samples. A/B/C/D was represented the relative concentrations of samples under various depuration periods - 0/1/5/9 days; Different metabolites were screened out according to VIP values (VIP>1.5) in the OPLS-DA models and p value in t-test (p<0.05); *: The statistical power was bigger than 0.8.*

NO	Name	MW (Da)	Retention time(min)	Relative amount		
				B/A	C/A	D/A
1	Urea	60.03	15.540	0.227*	0.039*	0.051*
2	Pyruvate	88.02	18.223	0.657*	0.543*	0.549*
3	Oxalic acid	90.00	18.223	0.668	0.539*	0.524*
4	Isovaleric acid	102.07	15.529	0.116*	0.032*	0.038*
5	Ribitol	152.07	15.530	0.117*	0.023*	0.026*
6	Citrulline	175.10	15.530	0.110*	0.014*	0.015*
7	Retinol	286.23	13.745	0.457*	0.355*	0.513*
8	Stearic acid	284.27	13.002	0.490*	0.498*	0.595*
9	Vitamin D3	384.34	15.671	0.391*	0.106*	0.145*
10	LysoPE(0:0/20:0)	509.35	11.536	1.285	1.246	1.539*
11	Thymine	126.04	0.978	0.777		0.668
12	TXB2	370.24	14.021	0.756*		0.661*
13	LysoPE(0:0/22:2(13Z,16Z))	533.35	11.856	1.611		1.648*
14	LysoPE(0:0/22:1(13Z))	535.36	12.322	1.441		1.565*
15	Succinic acid	118.03	18.186		0.662*	0.716*
16	Creatine	131.07	3.443		4.482*	4.182*
17	Ornithine	132.09	3.471		6.264*	6.017*
18	Caprylic acid	144.12	1.884		7.820*	4.425*
19	L-Tyrosine	181.07	3.446		4.278*	4.018*
20	D-Sorbitol	182.08	11.463		2.768*	2.925*
21	L-Cystathionine	222.07	11.391		2.870*	3.090*
22	L-Tryptophan	204.09	11.209		0.391*	0.541*
23	Myristic acid	228.21	11.595		0.484*	0.651*
24	Guanosine	283.09	3.460		7.524*	6.447*
25	Argininosuccinic acid	290.12	18.117		1.834	1.766*
26	β-estradiol	272.18	0.953		3.156*	2.703
27	Alpha-CEHC	278.15	11.442		2.593*	2.751*
28	Cortisone	360.19	11.455		1.756*	1.880*
29	Adenosine monophosphate	347.06	0.867		3.489*	1.869
30	PGA1	336.23	11.447		0.416*	0.554*
31	Nutriacholic acid	390.28	14.222		0.490*	0.537*
32	MG(0:0/22:5(4Z,7Z,10Z,13Z,16Z)/0:0)	404.29	13.096		0.603*	0.610
33	Vitamin D2	396.34	10.260		2.702*	2.869*

34	LysoPE(0:0/14:0)	425.25	9.817	0.491*	0.550*
35	LysoPE(0:0/18:3(6Z,9Z,12Z))	475.27	10.080	1.324*	1.556*
36	LysoPE(0:0/18:2(9Z,12Z))	477.29	10.467	1.348	1.509*
37	LysoPE(0:0/20:4(5Z,8Z,11Z,14Z))	501.29	10.522	1.247*	1.510*
38	PE(14:0/18:2(9Z,12Z))	687.48	14.375	0.590	0.358*
39	PC(14:0/P-16:0)	689.54	14.707	0.474*	0.329*
40	PE(14:0/20:5(5Z,8Z,11Z,14Z,17Z))	709.47	14.065	0.531	0.490*
41	PE(14:0/20:3(5Z,8Z,11Z))	713.50	14.521	0.571	0.424*

604
605

Table 3 KEGG Metabolism Pathway of DEGs in the flesh of carp during different STMFPS treatments

Pathway	The number of DEGs			All-gene	Pathway ID	Level 1
	Ctr vs. 1 d	Ctr vs. 5 d	Ctr vs. 9 d			
Metabolic pathways	503	1163	1040	4521	ko01100	Global and overview maps
Purine metabolism	83	194	168	807	ko00230	Nucleotide metabolism
Pyrimidine metabolism	61	136	118	440	ko00240	Nucleotide metabolism
Glycerophospholipid metabolism	44	107	92	424	ko00564	Lipid metabolism
Lysine degradation	41	91	89	371	ko00310	Amino acid metabolism
N-Glycan biosynthesis	49	87	72	227	ko00510	Glycan biosynthesis and metabolism
Oxidative phosphorylation	28	87	52	332	ko00190	Energy metabolism
Inositol phosphate metabolism	40	80	82	345	ko00562	Carbohydrate metabolism
Carbon metabolism	33	78	78	393	ko01200	Global and overview maps
Glycerolipid metabolism	24	62	51	206	ko00561	Lipid metabolism
Sphingolipid metabolism	25	61	44	204	ko00600	Lipid metabolism
Amino sugar and nucleotide sugar metabolism	19	56	43	188	ko00520	Carbohydrate metabolism
Arginine and proline metabolism	18	53	43	224	ko00330	Amino acid metabolism
Cysteine and methionine metabolism	19	52	41	192	ko00270	Amino acid metabolism
Ether lipid metabolism	24	49	43	191	ko00565	Lipid metabolism
Arachidonic acid metabolism	19	47	39	205	ko00590	Lipid metabolism
Biosynthesis of amino acids	20	47	39	213	ko01230	Global and overview maps
Glutathione metabolism	13	45	44	194	ko00480	Metabolism of other amino acids
Mannose type O-glycan biosynthesis	28	38	41	97	ko00515	Glycan biosynthesis and metabolism
Glycolysis / Gluconeogenesis	13	38	0	196	ko00010	Carbohydrate metabolism
Other types of O-glycan biosynthesis	23	37	39	108	ko00514	Glycan biosynthesis and metabolism
Pyruvate metabolism	13	35	38	174	ko00620	Carbohydrate metabolism
Fatty acid metabolism	13	34	34	185	ko01212	Global and overview maps
Retinol metabolism	15	33	31	146	ko00830	Metabolism of cofactors and vitamins
Porphyrin and chlorophyll metabolism	14	33	28	97	ko00860	Metabolism of cofactors and vitamins
Valine, leucine and isoleucine degradation	13	33	28	116	ko00280	Amino acid metabolism
Tryptophan metabolism	10	32	33	118	ko00380	Amino acid metabolism
Fructose and mannose metabolism	10	32	32	116	ko00051	Carbohydrate metabolism

Glycosaminoglycan biosynthesis - heparan sulfate / heparin	14	31	30	116	ko00534	Glycan biosynthesis and metabolism
Drug metabolism - cytochrome P450	7	30	30	125	ko00982	Xenobiotics biodegradation and metabolism
Glycosphingolipid biosynthesis - lacto and neolacto series	10	28	27	124	ko00601	Glycan biosynthesis and metabolism
Alanine, aspartate and glutamate metabolism	11	28	25	122	ko00250	Amino acid metabolism
Nicotinate and nicotinamide metabolism	9	27	28	112	ko00760	Metabolism of cofactors and vitamins
Drug metabolism - other enzymes	15	26	29	130	ko00983	Xenobiotics biodegradation and metabolism
Metabolism of xenobiotics by cytochrome P450	10	26	28	124	ko00980	Xenobiotics biodegradation and metabolism
Citrate cycle (TCA cycle)	7	26	25	143	ko00020	Carbohydrate metabolism
One carbon pool by folate	11	25	28	156	ko00670	Metabolism of cofactors and vitamins
Other glycan degradation	13	25	24	60	ko00511	Glycan biosynthesis and metabolism
Glyoxylate and dicarboxylate metabolism	8	24	34	132	ko00630	Carbohydrate metabolism
Steroid hormone biosynthesis	12	24	26	133	ko00140	Lipid metabolism
Pentose phosphate pathway	13	24	19	95	ko00030	Carbohydrate metabolism
Glycosaminoglycan biosynthesis- chondroitin sulfate/dermatan sulfate	12	24	18	105	ko00532	Glycan biosynthesis and metabolism
Drug metabolism - cytochrome P450	7	30	30	125	ko00982	Xenobiotics biodegradation and metabolism
Glycosphingolipid biosynthesis - lacto and neolacto series	10	28	27	124	ko00601	Glycan biosynthesis and metabolism
Alanine, aspartate and glutamate metabolism	11	28	25	122	ko00250	Amino acid metabolism
Nicotinate and nicotinamide metabolism	9	27	28	112	ko00760	Metabolism of cofactors and vitamins
Drug metabolism - other enzymes	15	26	29	130	ko00983	Xenobiotics biodegradation and metabolism
Metabolism of xenobiotics by cytochrome P450	10	26	28	124	ko00980	Xenobiotics biodegradation and metabolism
Citrate cycle (TCA cycle)	7	26	25	143	ko00020	Carbohydrate metabolism
One carbon pool by folate	11	25	28	156	ko00670	Metabolism of cofactors and vitamins

Other glycan degradation	13	25	24	60	ko00511	Glycan biosynthesis and metabolism
Glyoxylate and dicarboxylate metabolism	8	24	34	132	ko00630	Carbohydrate metabolism
Steroid hormone biosynthesis	12	24	26	133	ko00140	Lipid metabolism
Pentose phosphate pathway	13	24	19	95	ko00030	Carbohydrate metabolism
Glycosaminoglycan biosynthesis - chondroitin sulfate / dermatan sulfate	12	24	18	105	ko00532	Glycan biosynthesis and metabolism
Mucin type O-glycan biosynthesis	13	23	21	119	ko00512	Glycan biosynthesis and metabolism
Fatty acid degradation	10	23	16	132	ko00071	Lipid metabolism
Glycosylphosphatidylinositol (GPI)-anchor biosynthesis	12	22	26	85	ko00563	Glycan biosynthesis and metabolism
Glycine, serine and threonine metabolism	7	22	25	114	ko00260	Amino acid metabolism
Terpenoid backbone biosynthesis	12	22	21	54	ko00900	Metabolism of terpenoids and polyketides
Galactose metabolism	5	19	14	113	ko00052	Carbohydrate metabolism
Pentose and glucuronate interconversions	8	18	20	79	ko00040	Carbohydrate metabolism
Tyrosine metabolism	7	18	19	90	ko00350	Amino acid metabolism
Propanoate metabolism	11	18	17	90	ko00640	Carbohydrate metabolism
Starch and sucrose metabolism	4	18	17	128	ko00500	Carbohydrate metabolism
Selenocompound metabolism	8	17	12	39	ko00450	Metabolism of other amino acids
alpha-Linolenic acid metabolism	8	17	10	91	ko00592	Lipid metabolism
Fatty acid elongation	3	15	18	92	ko00062	Lipid metabolism
Glycosphingolipid biosynthesis - globo and isoglobo series	4	15	14	69	ko00603	Glycan biosynthesis and metabolism
Linoleic acid metabolism	6	15	12	88	ko00591	Lipid metabolism
Histidine metabolism	5	14	12	53	ko00340	Amino acid metabolism
beta-Alanine metabolism	12	13	19	86	ko00410	Metabolism of other amino acids
Ascorbate and aldarate metabolism	6	13	17	70	ko00053	Carbohydrate metabolism
Fatty acid biosynthesis	5	13	16	68	ko00061	Lipid metabolism
Pantothenate and CoA biosynthesis	8	13	14	53	ko00770	Metabolism of cofactors and vitamins
Glycosphingolipid biosynthesis-ganglio series	5	13	13	73	ko00604	Glycan biosynthesis and metabolism
Glycosaminoglycan degradation	4	12	19	62	ko00531	Glycan biosynthesis and metabolism
Butanoate metabolism	5	12	11	48	ko00650	Carbohydrate metabolism
Folate biosynthesis	1	12	11	45	ko00790	Metabolism of cofactors and vitamins
Sulfur metabolism	3	12	9	38	ko00920	Energy metabolism
Primary bile acid biosynthesis	7	11	14	57	ko00120	Lipid metabolism
Biosynthesis of unsaturated fatty acids	4	11	13	79	ko01040	Lipid metabolism
Glycosaminoglycan biosynthesis - keratan sulfate	4	11	13	91	ko00533	Glycan biosynthesis and metabolism

|						
Steroid biosynthesis	3	11	8	56	ko00100	Lipid metabolism
Thiamine metabolism	2	11	7	50	ko00730	Metabolism of cofactors and vitamins
Phenylalanine metabolism	7	10	12	42	ko00360	Amino acid metabolism
Ubiquinone and other terpenoid-quinone biosynthesis	3	10	11	30	ko00130	Metabolism of cofactors and vitamins
Arginine biosynthesis	3	10	9	64	ko00220	Amino acid metabolism
Riboflavin metabolism	6	10	8	24	ko00740	Metabolism of cofactors and vitamins
Phosphonate and phosphinate metabolism	2	9	10	71	ko00440	Metabolism of other amino acids
2-Oxocarboxylic acid metabolism	1	7	5	54	ko01210	Global and overview maps
Taurine and hypotaurine metabolism	4	6	8	42	ko00430	Metabolism of other amino acids
Vitamin B6 metabolism	2	5	7	16	ko00750	Metabolism of cofactors and vitamins
Synthesis and degradation of ketone bodies	1	4	5	13	ko00072	Lipid metabolism
Phenylalanine, tyrosine and tryptophan biosynthesis	2	4	4	18	ko00400	Amino acid metabolism
Valine, leucine and isoleucine biosynthesis	0	4	2	11	ko00290	Amino acid metabolism
Nitrogen metabolism	1	3	11	56	ko00910	Energy metabolism
D-Glutamine and D-glutamate metabolism	1	3	3	16	ko00471	Metabolism of other amino acids
Monobactam biosynthesis	1	3	1	7	ko00261	Biosynthesis of other secondary metabolites
Biotin metabolism	1	2	2	9	ko00780	Metabolism of cofactors and vitamins
Insect hormone biosynthesis	1	2	2	14	ko00981	Metabolism of terpenoids and polyketides
C5-Branched dibasic acid metabolism	0	2	0	6	ko00660	Carbohydrate metabolism
Lipoic acid metabolism	0	1	2	8	ko00785	Metabolism of cofactors and vitamins
Caffeine metabolism	2	1	1	8	ko00232	Biosynthesis of other secondary metabolites
D-Arginine and D-ornithine metabolism	0	1	1	6	ko00472	Metabolism of other amino acids
Neomycin, kanamycin and gentamicin biosynthesis	1	1	1	13	ko00524	Biosynthesis of other secondary metabolites
Polyketide sugar unit biosynthesis	0	1	0	2	ko00523	Metabolism of terpenoids and polyketides

608

609

610   Table 4: DEGs related to ornithine cycle in crucian carp muscle during depuration

Genetic code	Pathway No.	DEGs[a]			Expression of enzymes	Metabolites
		1 d	5 d	9 d		
109070501	k01940	+1.0	+2.7	ND	argininosuccinate synthase [EC:6.3.4.5]	citruline to arginosuccinate
109058290	k21121	ND	+1.4	+1.2	N-alpha-acetyltransferase 60 [EC:2.3.1.259]	glutamate to N-acteyl-glutamate
109045545	k01755	ND	+1.7	+1.0	argininosuccinate lyase [EC:4.3.2.1]	arginosuccinate to arginine
109056660	k12657	+1.2	+1.8	+1.4	delta-1-pyrroline-5-carboxylate synthetase [EC:2.7.2.11]/[1.2.1.41]	glutamate to glutamate 5-semialdehyde
109088420	k00819	ND	-2.1	-2.3	ornithine--oxo-acid transaminase [EC:2.6.1.13]	ornithine to glutamate 5-semialdehyde
109113777	k00286	ND	+1.3	+1.3	pyrroline-5-carboxylate reductase [EC:1.5.1.2]	proline to 1-pyrroline-5-carboxylate
109054371	k11540	ND	+1.1	+1.1	carbamoyl-phosphate synthase [EC:6.3.5.5]	glutamine to carbomyl-phosphate

611   (Note, [a] value is presented as the differential expression multiple after log2 conversion. Positive value indicates
612   that the sample group was up-regulated compared with the control group (depurated for 0 day). Negative value shows
613   that the sample group was down-regulated compared with the control group (depurated for 0 day).)
614
615
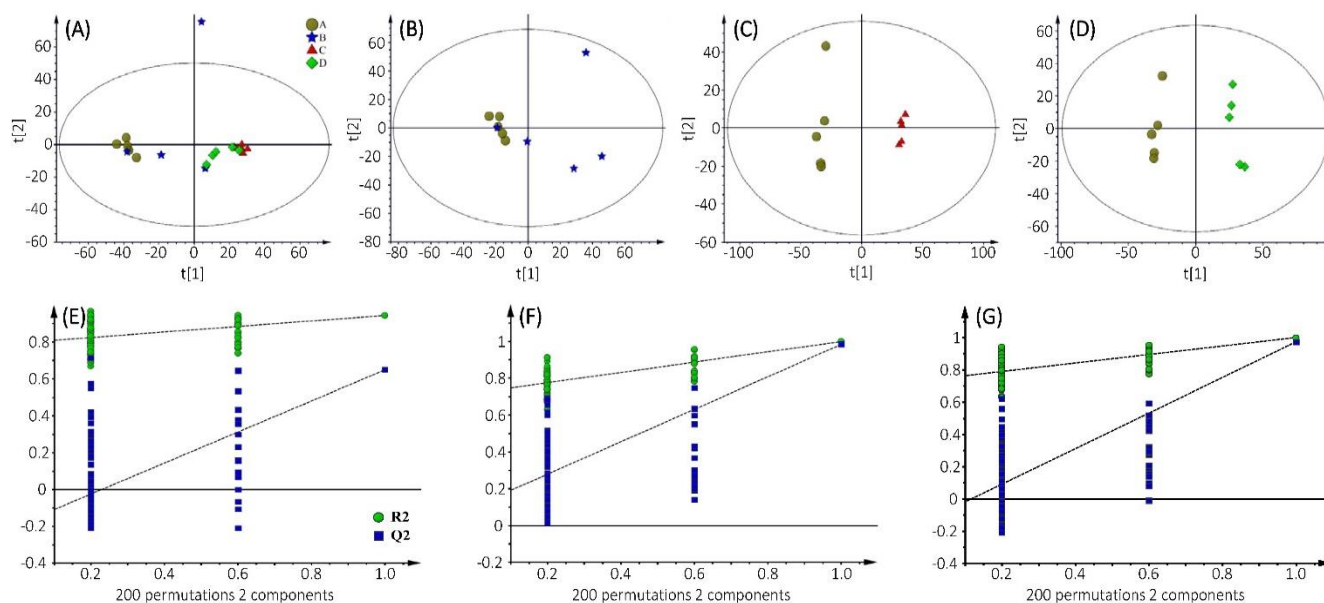
632   **Fig. 1** Results of PCA analysis (A-D) and the permutation test plots (E-G) from the OPLS-DA

633   models for the metabolites obtained from crucian carp muscle during different depuration periods

634   and detected using UPLC-QTOF/MS in both ionization modes. *Note: A: All samples in four*

635   *groups; B: Control group vs. 1 d group; C: Control group vs. 5 d group; D: Control group vs. 9 d*

636   *group; E: Control group vs. 1 d group; F: Control group vs. 5 d group; G: Control group vs. 9 d*

637   *group. The criteria for validity of the OPLS-DA model are indicated as following: All blue Q^2-*

638   *values to the left are lower than the original points to the right; or the blue regression line of the*

639   *Q^2-pints intersected the vertical axis (on the left) or below zero.*

640

641
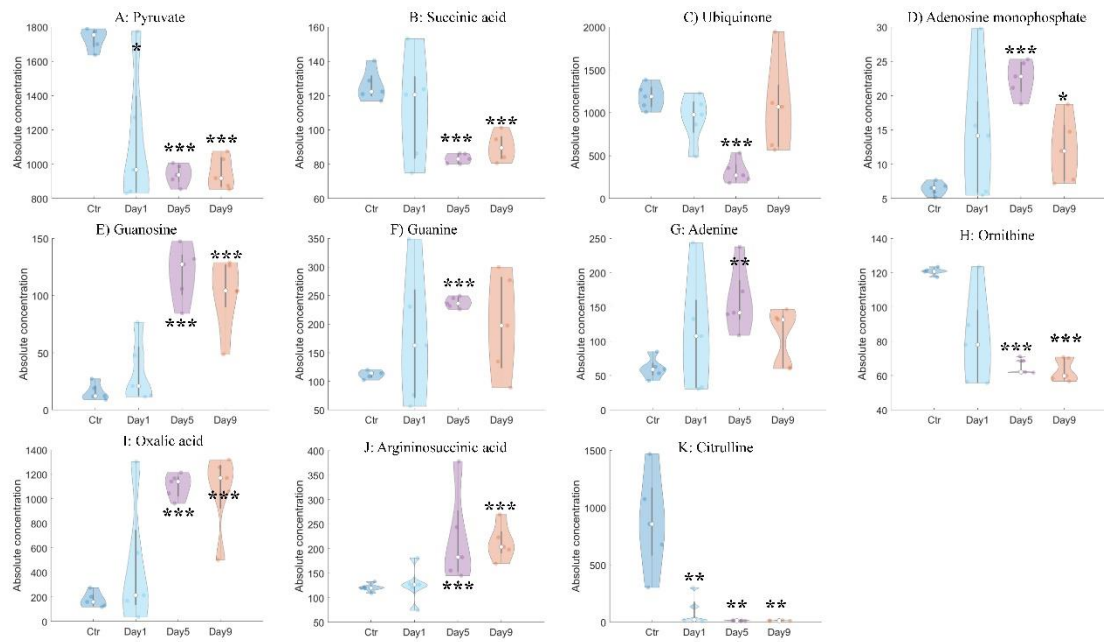
Fig. 2: Comparative contents of different metabolites in crucian carp muscle during the depuration
procedure ("*": <0.05; "**": p<0.01; "***": p<0.001). Note: A-D: Related with energy metabolism;
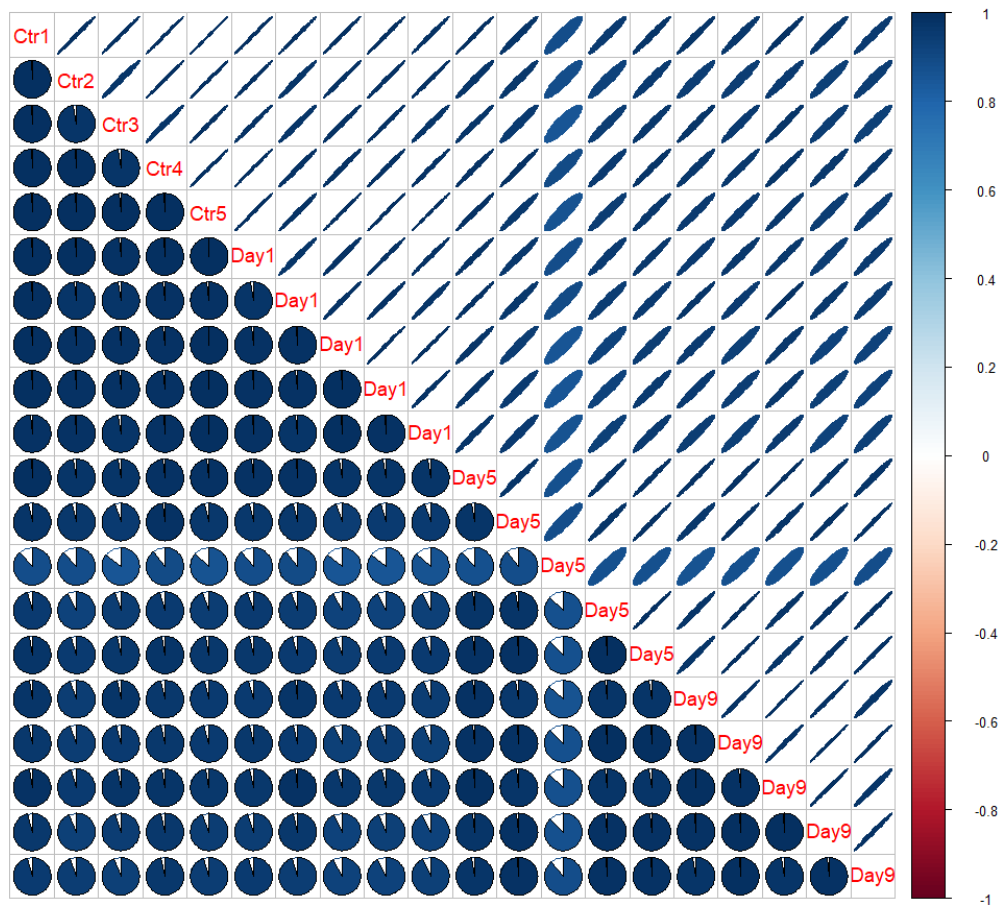E-H: Related with the purine metabolic cycle; I-K: Related with the ornithine metabolic cycle.

645

646
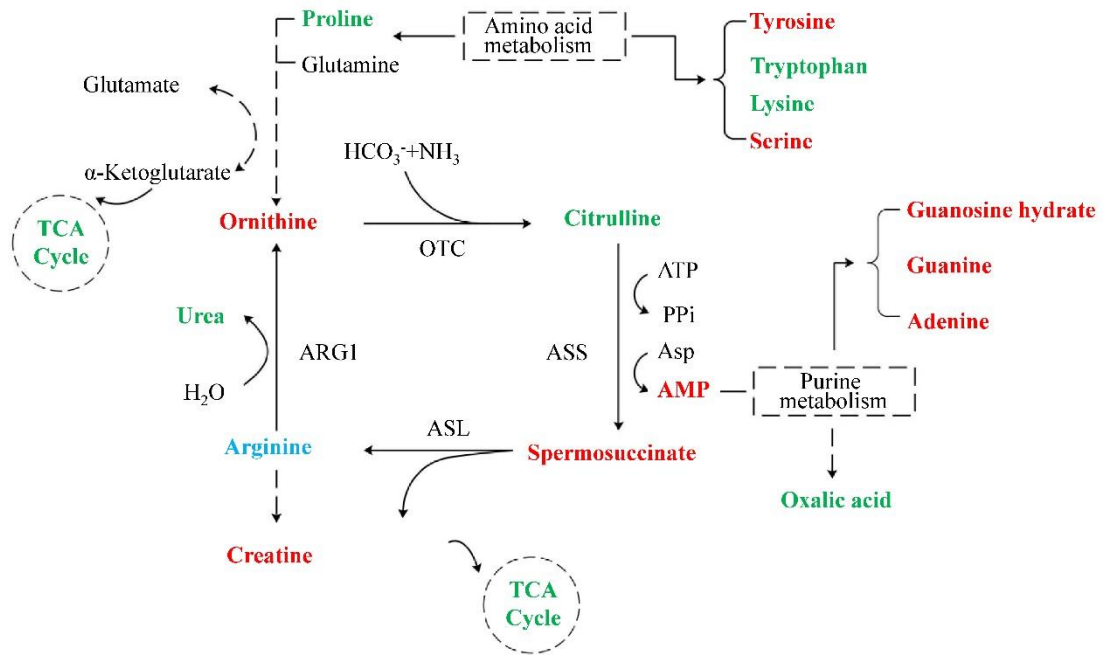
Fig. 3 Effect of depuration on metabolic pathways of crucian carp muscle. Note: *Different colors of metabolites represent change of comparative content, red: increased; blue: did not significantly change; green: decreased.*

Fig. 4 Correlation heatmap of the Pearson correlation coefficient of all gene expressions in four different groups (Ctr1-Ctr5: Control; Day1: 1 d; Day5: 5 d; Day9: 9 d).

655
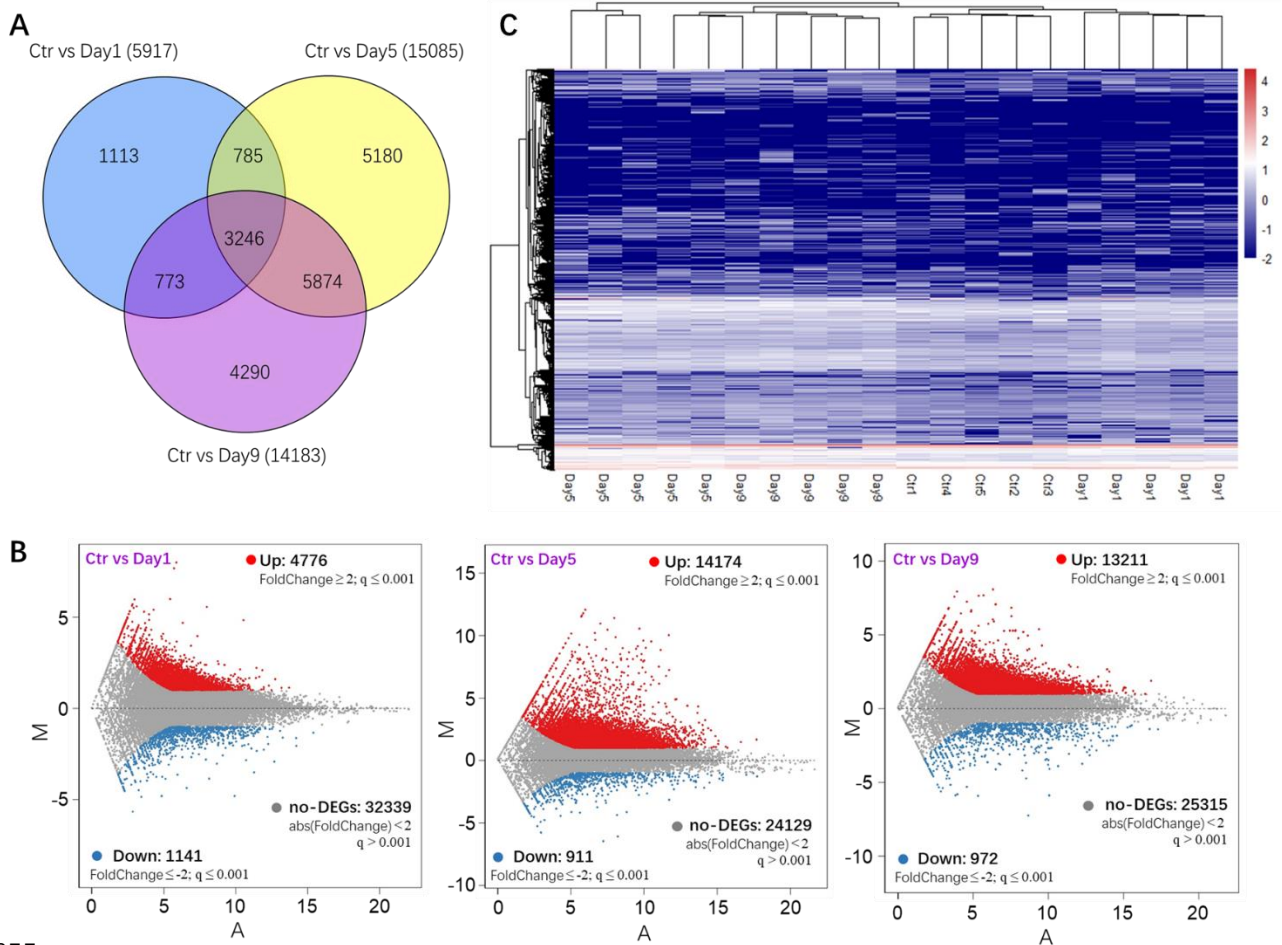
Fig. 5 (A) Venn diagram of significantly enriched DEGs in different group comparisons representing the unique and overlapping DEGs. (B) MA plot distribution of DEGs of crucian carp muscle during different deputation periods. The red and blue dots indicate that the genes were differently expressed and the grey dots illustrate that the genes were not differentially expressed. The positive and negative values represent the up- and downregulation of DEGs, respectively. (C) Clustered heatmap for DEGs detected from different groups with rows representing DEGs and columns representing samples. *Note: Columns represent every gene set that was significantly up-regulated (red) or down-regulated (blue) in different groups (Ctr1-Ctr5: Control; Day1: 1 d; Day5: 5 d; Day9: 9 d).*
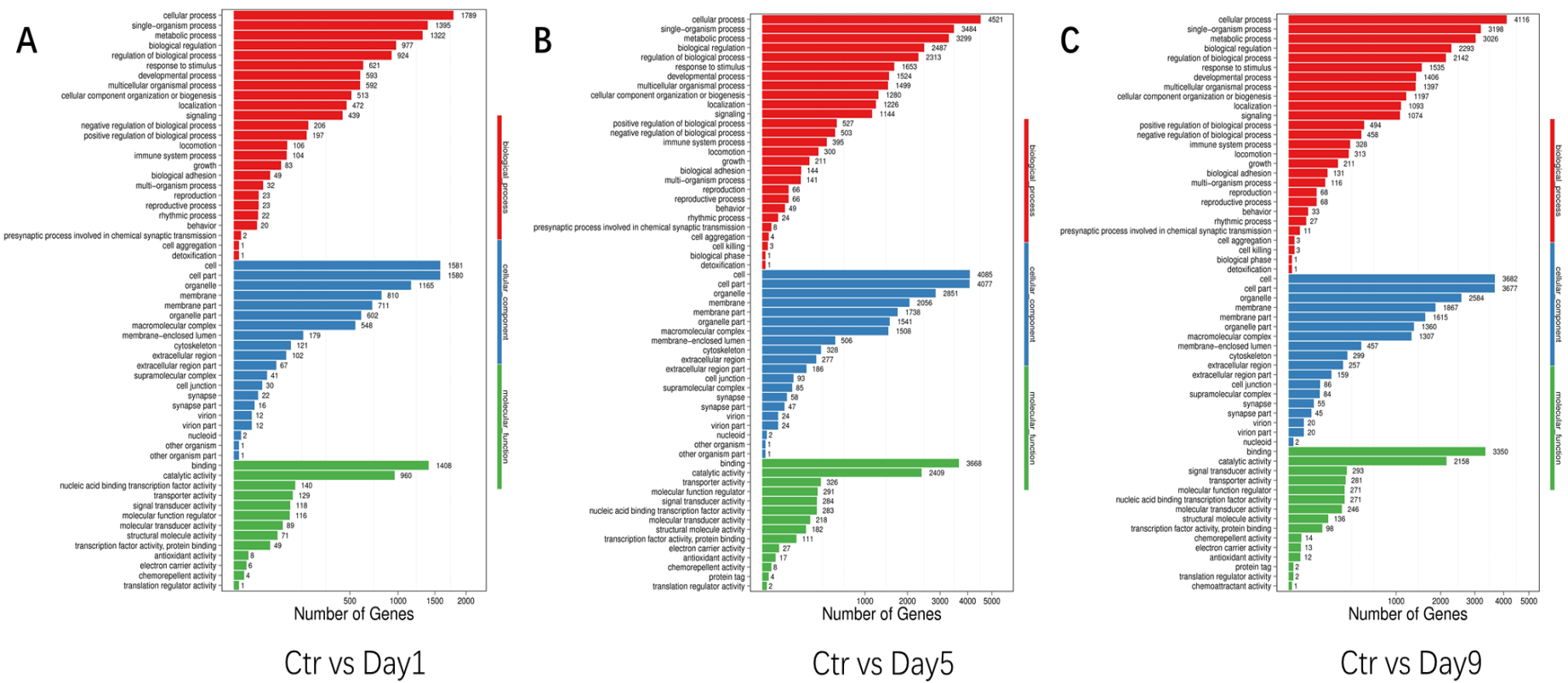
664

Fig. 6 GO classification of DEGs. (A) GO functional classification of DEGs between the control (Ctr) and Day1. (B) GO functional classification of DEGs between Ctr and Day5. (C) GO functional classification of DEGs between the Ctr and Day9. (Ctr, Day1, Day5, Day9 represent 0 d, 1 d, 5 d and 9 d STMFPS treated groups, respectively).